

S 1. Methods for parameter estimation in one- and two-parameter probability distributions

One- and two-parameter distributions were chosen as reference for evaluating overparameterization and overfitting in more complex models. For this purpose, the exponential (Exp) and two-lognormal (2LN) distributions were selected.

The exponential distribution (Exp) was used in the research of (Balbi and Lallemand, 2023; Ekanayake and Cruise, 1993), (Willems et al., 12–14 November). The PDF function is given by equation (1):

$$f(x) = \lambda e^{-\lambda x}, \text{ for } x \geq 0 \quad (1)$$

10 where:

λ is the rate.

Estimation of the parameters and fitting of the Exp distribution was carried out using the following R packages: ‘stats’.

The 2-parameter lognormal distribution (2LN) was used in the research of (Kuczera, 1982), (Willems et al., 2007), Cassalho et al. (2018), The PDF function is given by equation (2):

$$f(x) = \frac{1}{\sqrt{2\pi\sigma x}} e^{-\frac{(\log(x)-\mu)^2}{2\sigma^2}}, \quad (2)$$

where: μ and σ are the mean and standard deviation of the logarithm, respectively.

20 The estimation of the parameters and fitting of the 2LN distribution was carried out using the following R packages: ‘stats’.

S 2. Goodness-of-fit assessment for one- and two-parameter distributions

The goodness of fit was assessed using the MAE or RMSE accuracy measures (for details see subsection 3.4) between two distributions: Exp and LN2. Additionally, both distributions (Exp and LN2) were evaluated against three- and four-parameter distributions (P3, LN3, GEV and GGEV) using the same criteria.

S 3. Random distributions

30 Random distributions were generated for the GEV, GGEV, LN2, and Exp distributions. Using the 'MCMCExtreme' package, we used random generation from the GGEV distribution: `rggev(n, shape, location, scale, additional shape)` to create random samples of the GGEV distribution. Sample size (n) corresponded to the empirical sample size. We used the parameters (shape, location, scale, additional shape) determined for the theoretical GGEV distribution. Of course, we did this only for the best-fit samples to the GGEV distribution (281 samples). Next, we obtained new data series, which we called random series.

Using the 'evir' package, we generated random samples from the GEV distribution using the function `rgev(n, shape, location, scale)`. The sample size (n) was based on the empirical sample size. We applied the parameters (shape, location, scale) that were determined for the theoretical GEV distribution. This process was conducted exclusively for the 172 best-fit samples to the
40 GEV distribution. Next, we created new data series, which we referred to as the random series.

Using the 'stats' package (functions `rlnorm` and `rexp`), random distributions were generated based on the parameters of the theoretical LN2 and Exp distributions.

The `set.seed` (123) was used for generated random samples so that the results could be reproduced.

Table S1. The count of four fitting distributions (P3, LN3, GEV, GGEV) using mean absolute error accuracy measure, categorized by types of trends

Goodness of fit distribution	Mann Kendall trend test	P3	LN3	GEV	GGEV	Sum
Mean absolute error	No trend	96	61	111	178	446
Mean absolute error	Negative trend	32	27	53	88	200
Mean absolute error	Positive trend	4	5	8	15	32
	Sum	132	93	172	281	678

Explanation to the table: P3 – Pearson type III distribution, LN3 – 3-parameters log-normal distribution, GEV – Generalized extreme value distribution, GGEV – Dual Gamma Generalized Extreme Value Distribution

Table S2. Probability distributions (P3, LN3, GEV, GGEV) for samples classified by catchment area size: micro-catchments (0-10 km²), meso-catchments (10-100 km²), macro-catchments (100-1,000 km²), large catchments (1,000-10,000 km²), and very large catchments (>10,000 km²).

Catchment area	P3	LN3	GEV	GGEV	Total
Monotonic trend					
<10	0	0	2	0	2
10-100	9	8	20	11	48
100-1,000	46	30	62	120	258
1,000-10,000	31	17	18	39	105
>10,000	10	6	9	6	32
Negative trend					
<10	0	0	0	0	0
10-100	1	2	3	2	8
100-1,000	14	14	31	50	109
1,000-10,000	13	7	15	27	62
>10,000	4	4	3	7	18
Positive trend					
<10	0	0	0	0	0
10-100	1	1	3	6	11
100-1,000	3	4	4	7	18
1,000-10,000	0	0	1	2	3
>10,000	0	0	0	0	0

Explanation to the table: P3 – Pearson type III distribution, LN3 – 3-parameters log-normal distribution, GEV – Generalized extreme value distribution, GGEV – the Dual Gamma Generalized Extreme Value Distribution

Table S3. Basic characteristics of the catchment area size (A) and peak flow (Qp) for descriptive monotonic trend samples with determined probability distributions

No.	Probability distribution	Trend detection	A [km ²]		Qp [m ³ /s]	
			Min	Max	Min	Max
1	3P3	NMT	33	193,666	1.94	6,950
2	LN3	NMT	36	109,775	8.64	6,160
3	GEV	NMT	3.6	168,239	1.64	6,980
4	GGEV	NMT	50	68,216	2.18	6,000

Table S4. Basic characteristics of the catchment area size (A) and maximum extreme flow magnitude (WWQ) for descriptive negative trend samples with determined probability distributions

No.	Probability distribution	Trend detection	A[km ²]		Qp [m ³ /s]	
			Min	Max	Min	Max
1	3P3	NT	58	32 092	6.08	972
2	LN3	NT	68	30 648	6.56	1480
3	GEV	NT	49	38 395	4.46	2400
4	GGEV	NT	83	180 267	4.97	6890

Table S5. Basic characteristics of the catchment area size (A) and maximum extreme flow magnitude (WWQ) for descriptive positive trend samples with determined probability distributions

Probability distribution	Trend detection	A [km ²]		Qp [m ³ /s]	
		Min	Max	Min	Max
3P3	PT	34	583	10.7	464
LN3	PT	96	376	29.4	371
GEV	PT	48	2 470	4.55	235
GGEV	PT	35	1 480	8.29	780

70

S4. Detailed description of the Impact of Environmental Factors on the Probability Distribution Parameters

Redundancy analysis is well-suited for examining relationships between sets of variables, enabling the assessment of whether environmental factors have a similar impact on the parameters of different distributions. RDA was performed separately for each distribution (GEV, GGEV, LN3, P3).

80 The independent variables are catchment area ranges: a – micro-catchments, b – meso-catchments, c – macro-catchments, d – large catchments, e – very large catchments; flow peak (Qp); trend (NMT is no trend, PT is positive trend and NT is negative trend); the nature of the watercourse (L – lowlands, H – highlands, M – mountains); empirical skewness (Skewn.), and 4th center moment (4thMoment); empirical kurtosis (Kurt.), sample size (N) (Fig. S1a- S1d). The response variables are add. shape (Fig. S1), location, scale, and shape (Fig. S1-S4, Table S3),

Since the mean, standard deviation, variance, third moment, and 4thMoment are interrelated, it is essential to carefully select the set of explanatory variables. It was also confirmed that multicollinearity exists between skewness and kurtosis as explanatory variables (Variance Inflation Factor, VIF > 10). Collinearity between skewness and kurtosis may result from the fact that both of these measures are defined using standard deviation (SD). Therefore, RDA was conducted separately for kurtosis (Fig. S1a, S2a, S3a, S4a) and skewness (Fig. S1b, S2b, S3b, S4b). Additionally, RDA was performed with the
90 inclusion of catchment area ranges and Kurt. was replaced with the 4thMoment and Skewn (see Figures S1c, S2c, S3c, and S4c).

The decision to replace Kurt. with the 4th Moment was made because both Skewn. and Kurt. are functions of standard deviation, making them potentially collinear. The use of the Skewn. and the 4thMoment allows for capturing more detailed aspects of the data distribution. The 4thMoment measures the overall Kurt. (that is, how heavy the tails of the distribution are), while Kurt. is the normalized version of this moment. Following the initial RDA, subsequent analyses considered only the changes that were not identified in the first analysis. A detailed description of the RDA analyses for the distributions is provided in the supplementary materials (Section S4).

100 The use of topography in modeling Qp helps to uncover the runoff mechanism prevailing in the catchment (Valeo, 2013).

4.4.1 GGEV Distribution

The first two axes (RDA 1 and RDA 2) explain 54.00% of the variance (45.76% and 8.24%, respectively) (Fig. S1a). The Qp, and A are strongly correlated with RDA 1 and Kurt. is strongly correlated with RDA 2. According to the response variables, scale and location are related to RDA 1. Shape and Add shape are related to RDA 2. Scale and Location are strongly positively correlated with Qp (scores 0.95) and A (scores 0.94). The shape and Add shape are positively related to Kurt. (scores

0.90) The add. shape and shape are inversely proportional to N (scores -0.14). The H (scores -0.68), L (scores 0.70), M (scores -0.14) and PT (scores -0.33) and NT (scores 0.25) are correlated with RDA 3. Samples with NMT (scores 0.14) did not affect the distribution parameters for add shape and shape.

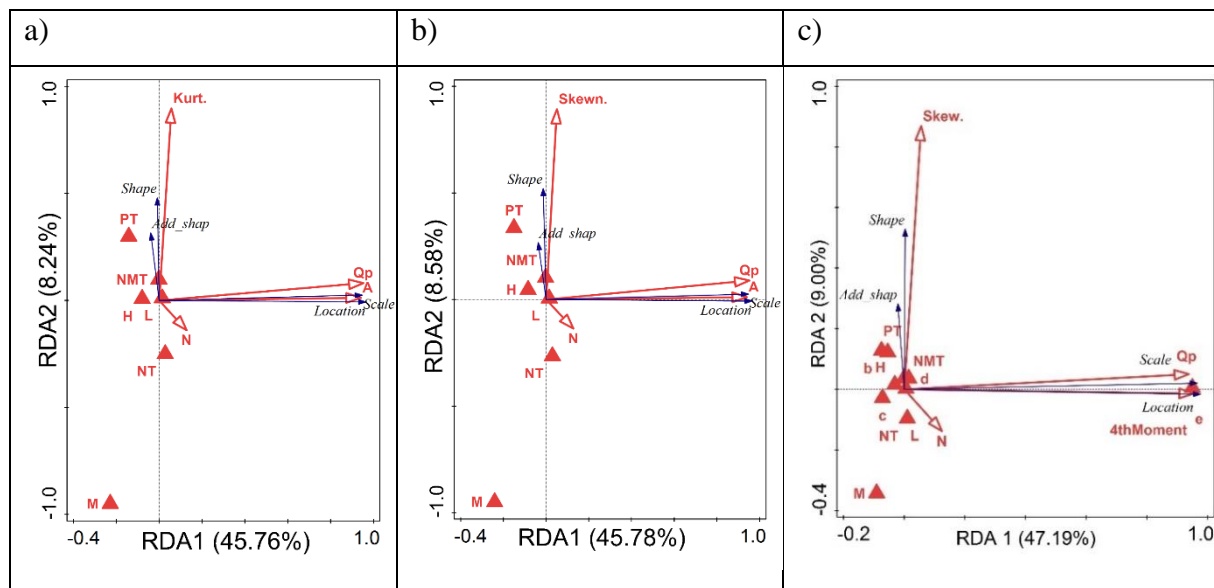


Fig. S1. Redundancy analysis (RDA) of the relation between environmental variables and sample characteristics and the parameters of GGEV (scale, shape, add. shape, location). Description of symbols: catchment area ranges (in km²): a – < 10, b – 10-100, c – 100-1000, d – 1000-10000, e – > 10000; flow peak (Q_p); trend (NMT is no trend, PT is positive trend and NT is negative trend); the nature of the watercourse (L – lowlands, H – highlands, M – mountains), parameters of the empirical sample (Skewn. is the empirical skewness, Kurt. is the empirical kurtosis and 4thMoment is the 4th center moment); sample size (N).

In the second RDA, the first two axes (RDA 1 and RDA 2) explain 54.36% of the variance (45.78% and 8.58%, respectively) (Fig. S1b). The Q_p, and A are strongly correlated with RDA 1 and Skewn. with RDA 2. According to the response variables, scale and location are related to RDA 1, and shape and add. shape are related to RDA 2. Scale and Location are strongly positively correlated with Q_p (scores 0.95) and A (scores 0.94). The shape and add. shape are positive related to Skewn. (0.89). The add. shape and shape are inversely proportional to N (-0.13). The H (scores -0.69), and L (scores 0.73) and PT (scores -0.29) are correlated with RDA 3. In turn, the M (scores 0.30) is correlated with RDA 4. Samples with NMT (scores 0.14) and NT (scores -0.18) did not affect the distribution parameters for add. shape and shape.

Both skewness and kurtosis, as shown in the graphs (Fig. S1a-b), are correlated with the shape and add. shape parameters, which may support the additional parameter mechanism described by the author et al. (2015) for this distribution.

In the third RDA the first two axes (RDA 1 and RDA 2) explain 56.19% of the variance (47.19% and 9%, respectively) (Fig. S1c). Thus, the explained variance is slightly higher compared to the previous

two canonical analyses for the GGEV distribution. The Qp, (e) and 4thMoment are strongly correlated with RDA 1 and so is Skew. with RDA 2.

According to the response variables, scale and location are related to RDA 1, and shape and add. shape are related to RDA 2. Scale is strongly positively correlated with Qp and location is strongly positively correlated with (e) and 4thMoment (Fig. S1b). This means that higher Qp values correspond to a larger scale parameter in the GGEV distribution. Larger catchment areas (e) lead to an increase in the location parameter, which shifts the central point of the distribution. As can be seen in the biplot (Fig. S1a) the Kurt. parameter affects the shape and add. shape, while the 4thMoment influences the location. Meanwhile, the third moment strongly correlates with the scale (not shown in the graph). An increase in the 4thMoment, which measures the concentration of values around the mean and is also related to Kurt., indicates an increase in the value of the location parameter. The location parameter determines where the center of the distribution is located on the number axis. The fact that the greater the 4thMoment, the higher the location parameter means that in a heavy-tailed distribution, where more extreme values occur, the central tendency of the distribution (measured by the location parameter) shifts towards these higher values to better reflect the influence of extremes on the distribution. This, in turn, means that higher values of the 4thMoment cause the central value or location of these extreme values to shift towards higher values. If the location parameter increases with the 4thMoment, then the center of the distribution shifts to the right on the number axis. In turn, the 3rd central moment correlates with the distribution parameter known as scale because the scale affects the magnitude of deviations from the mean, and the 3rd central moment measures precisely these deviations.

The shape is positive related to Skew. The add. shape and shape are inversely proportional to N (Fig. S1c). In practice, this might suggest that with larger N, the distribution becomes less extreme or lighter. The shape parameters likely adjust to reflect a more stable and less variable distribution as the amount of data increases. Shape and add. shape are negatively correlated with NT (Fig. S1c). This may indicate that in situations where there is a downward trend in the data, the distribution becomes less varied or more flattened. A weak correlation could suggest that the values of add. shape and shape may slightly decrease with a NT.

We observe that add. shape is not as strongly correlated with Skewn. as shape. Add. shape serves as a supplementary parameter, and the canonical analysis shown in Fig. S1a-b indicated that add. shape has similar properties to shape. Since the 4thMoment is not associated with RDA2, it will not directly influence shape and add. shape, or its impact will be limited for the samples examined (Fig. S1a). However, the 4thMoment used to determine Kurt. will cause Kurt. to strongly correlate with shape parameters (Fig. S1c).

Scale and location are negatively correlated with (c). NMT had weak effect on scale and location (Fig. S1c). Moreover, (b), (d), H, M, L and PT do not have influence to the distribution parameters (Fig. S1c). This suggests

that terrain topography does not have a direct impact on the parameters of the GGEV distribution. Additionally, it can be suggested that not all types of catchments influence the shaping of distribution parameters. Very large catchments (e) have a strong positive impact, while macro-catchments (c) have a weak influence, and there is no effect on the parameters of meso-catchments (b) and large catchments (d). This may be because distribution parameters affecting larger areas may not have as strong an impact on smaller catchments, where local effects dominate over the effects related to distribution parameters (Arnaud et al., 2011; Roodsari and Chandler, 2017). An additional advantage of the distribution is its weak sensitivity to trends. Only a NT affects the shape parameter and the additional shape parameter.

Shape is correlated with Skewn. and Kurt. of the empirical data. This means that this parameter (shape) influences the asymmetry and tail distribution of the empirical flow data, which is consistent with the description by (Nascimento et al., 2015).

Further, this implies that temporal trends such as NMT and NT do not affect the parameters of the GGEV distribution.

In conclusion, distribution parameters are more closely related to the hydrological characteristics of flows than to the geographic or temporal features.

The RDA analysis indicates that the GGEV distribution is anticipated to be the least sensitive to landscape forms and N.

4.4.2 GEV Distribution

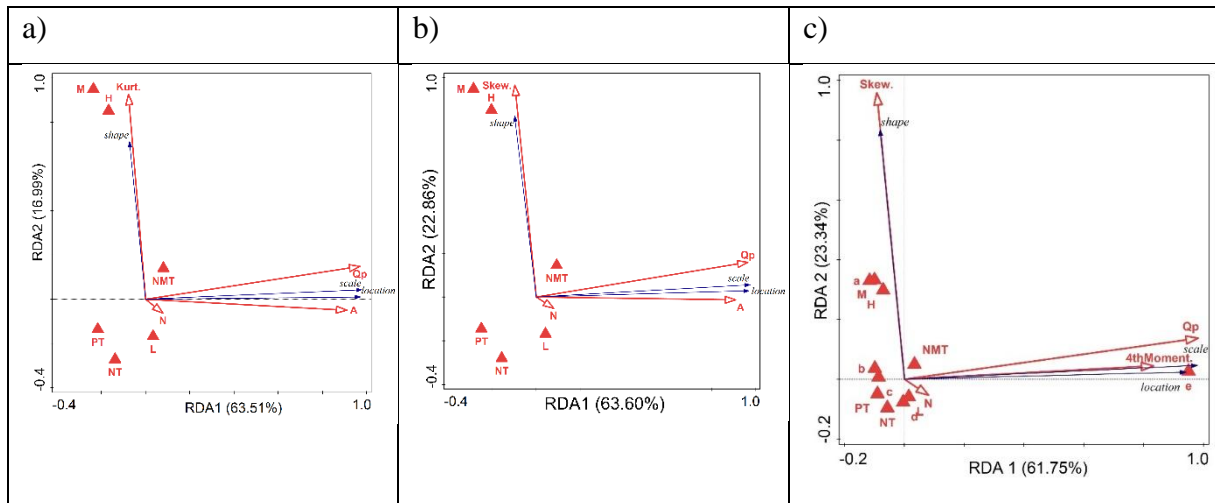


Fig. S2. Redundancy analysis (RDA) of the relation between environmental variables and sample characteristics and the parameters of GEV (scale, shape, location). Description of symbols: catchment area ranges (in km²): a – < 10, b – 10-100, c – 100-1000, d – 1000-10000, e – > 10000; flow peak (Q_p); trend (NMT is no trend, PT is positive trend and NT is negative trend); the nature of the watercourse (L – lowlands, H – highlands, M – mountains), parameters of the empirical sample (Skew. is the empirical skewness, Kurt. is the empirical kurtosis and 4thMoment is the 4th center moment); sample size (N).

The first two axes (RDA 1 and RDA 2) explain 80.50% of the variance (63.51% and 16.99%, respectively) (Fig. S2a). The Q_p, and A are strongly correlated with RDA 1 and so is Kurt. with RDA 2. According to the response variables, scale and location are related to RDA 1, and shape is related to

RDA 2. Scale and Location are strongly positively correlated with Qp (scores 0.96) and A (scores 0.91) (Fig. S2a). This is consistent with the findings of (Villarini and Smith, 2010). The shape is positively related to Kurt. (scores 0.93), H (scores 0.41), and M (scores 0.18), NMT (scores 0.22) (Fig. S2a). The shape is inversely proportional to L (scores -0.45) and NT (scores -0.21) (Fig. S2a). However, the shape parameter is more likely linked to hydrological processes and meteorological conditions than to the catchment area (He et al., 2015). The N (scores 0.14) is correlated with RDA 3 (Fig. S2a).

200 In the second RDA, the first two axes (RDA 1 and RDA 2) explain 54.36% of the variance (63.60% and 22.86%, respectively) (Fig. S2b). The Qp, and A are strongly correlated with RDA 1 and so is Skew. with RDA 2. According to the response variables, scale and location are related to RDA 1, and shape is related to RDA 2. Scale and Location are strongly positively correlated with Qp (scores 0.97) and A (scores 0.91) (Fig. S2b). What is particularly noteworthy is that the hydrological signatures related to flow magnitude, such as the location and scale parameters, are primarily dependent on A, which significantly influences their values, while other attributes have a lesser impact on the response variable. This is consistent with He et al. (2015), Northrop (2004), Tyralis et al. (2019). The shape is positively related to Skew. (scores 0.97), NMT (scores 0.20), H (scores 0.35), M (scores 0.15) (Fig. S2b). The shape is inversely proportional to NT (scores -0.19) and L (scores -0.39) (Fig. S2b). N (scores 0.13) is correlated with RDA 3. Scale and Location are inversely proportional to PT (scores -0.06) (Fig. S2b).

210 In the third RDA, the first two axes (RDA 1 and RDA 2) explain 85.09% of the variance (61.75% and 23.34%, respectively) (Fig. S2c). The Qp, e and 4thMoment are strongly correlated with RDA 1 and so is Skew. with RDA 2. According to the response variables, scale and location are related to RDA 1, and shape is related to RDA 2 (Fig. S2c). While it shows a strong correlation with the scale and location parameters, this relationship is not observed for the shape parameter (Tabari et al., 2021). The scale is strongly positively correlated with Qp (scores 0.98) and location is strongly positively correlated with e (scores 0.76) and 4thMoment (scores 0.83) (Fig. S2c). This is consistent with (Tabari et al., 2021), which report that the scale parameter of GEV, represents the deviation around the mean and serves as an indicator of the variance (Tabari et al., 2021). The location parameter indicates the center of the distribution and acts as an indicator of the mean (Tabari et al., 2021).

220 The shape is positively related to Skew. (scores 0.96) (Fig. S2c). The shape parameter determines the tail behavior of the distribution (He et al., 2015). Specifically, higher values of the shape parameter lead to heavier tails (Tabari et al., 2021; Tyralis et al., 2019; Villarini and Smith, 2010). The shape is negatively correlated with L (scores -0.39), NT (scores -0.19), and d (scores -0.11) (Fig. S2c). The scale and location are negatively correlated with PT (scores -0.05), c (-0.29). The NMT (scores 0.19) had a weak effect on shape. In turn, H (scores 0.35) and M (scores 0.15) had a weak relation to the shape (Fig. S2c). The shape parameter of GEV is correlated with nature (terrain elevation) (Sampaio and Costa, 2021; Tyralis et al., 2019). However, the morphologic characteristics of the catchments in the regression

model for the GEV shape parameter are small (Sampaio and Costa, 2021). Moreover, capturing the spatial variation of the GEV shape parameter by means of covariates, such as terrain elevation, remains a challenging task (Sampaio and Costa, 2021). On the other hand, (Ahilan et al., 2012) research confirms that the type of landscape affects the distribution of GEV. The shape parameter of GEV determines the behavior of the upper tail. Specifically, higher values of the shape parameter lead to heavier tails. The shape parameter's dependency is mainly influenced by climatic indices, while other catchment characteristics are less significant (Tyralis et al., 2019). This is consistent with He et al. (2015), who found no relationship between the shape parameter and the catchment area, which suggests that hydrological heterogeneity is implicitly captured by the shape parameter.

Moreover, N (scores 0.293), b (scores - 0.16) is related to RDA 3 (Fig. S2c).

RDA analysis confirms that the shape of the distribution are strongly dependent on the Skewn. of the empirical sample (Fig. S2b-c). The location parameter of GEV is positively correlated with the weight and the tail distribution in the empirical data.

When talking about the impact of catchment size on the GEV parameters, Villarini and Smith (Villarini and Smith, 2010) found that scale and location are positively correlated, while shape is negatively correlated. The magnitude of the shape parameter of GEV depends on the location of the gauge, whether it is in lowlands, highlands, or mountains (Villarini and Smith, 2010).

In sample (e), which is a very large catchment, the 4thMoment affects the location parameter and is strongly positively correlated with the location. In sample (c), the 4thMoment is weakly negatively correlated with the location and with PT. Landscape forms and trends, as well as catchment types (with the exception of micro-, meso-, and very large catchments), have a weak influence on the parameters of this distribution.

The scale parameter of GEV in the flood frequency analysis is strongly correlated with Q_p and MAF (Villarini and Smith, 2010). This relationship is further supported by the use of scale-invariant statistics, which show good correlations with historical flood-frequency records (Turcotte 1993). However, it is important to note that the scale parameter can vary over time, as demonstrated by the application of a non-stationary GEV model to account for changing streamflow series (Jiang 2019).

The shape parameter of GEV in the flood frequency analysis is a critical factor, but its determinants have been elusive (Tyralis 2019). While it is known to influence the upper tail of the distribution, its relationship with catchment attributes is not well understood. Morrison and Smith (2002) found that the shape parameter is not dependent on catchment morphological parameters or land cover properties, which suggests that other factors may be at play. Sampaio 2021 and Kumar 2003 both highlight the importance of GEV in regional flood frequency analysis, but do not specifically address the relationship between the shape parameter and the highlands area. Indeed, in their work (Northrop, 2004), they

analyze the relationship between the location, scale, and shape parameters of GEV, among other factors, of the annual maxima and catchment descriptors such as the area and base flow index. In this study, the MLE method was also used for estimating the distribution parameters. The work indicates a linear relationship between the location and scale parameters— as the catchment area increases, so do these parameters. Current research confirms this trend (Fig. S2a-b). On the other hand, regarding the shape parameter, Northrop (2004) states that there is no trend. Current studies show a negative trend, which is explained by Tyralis et al. (2019). According to Tyralis et al. (2019), the shape parameter exhibits a negative linear correlation with the catchment mean elevation. As the elevation increases, the value of the shape parameter slightly decreases (Fig. S2a-c).

4.4.3 Log-normal distribution (LN3)

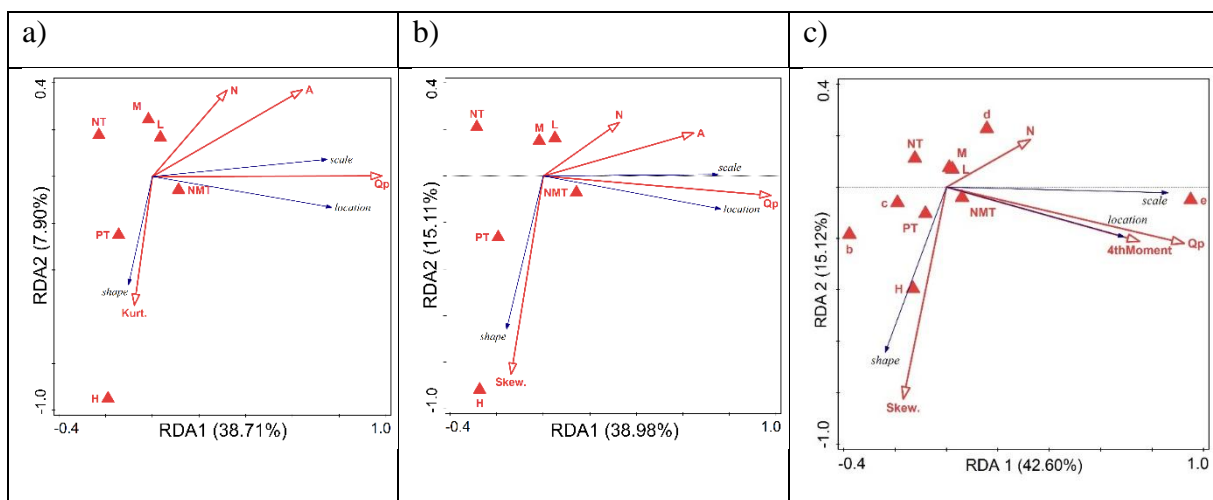


Fig. S3. Redundancy analysis (RDA) of the relation between environmental variables and sample characteristics and the parameters of LN3 (scale, shape, add. shape, location). Description of symbols: catchment area ranges (in km²): a – <10, b – 10-100, c – 100-1000, d – 1000-10000, e – > 10000; flow peak (Q_p); trend (NMT is no trend, PT is positive trend and NT is negative trend); the nature of the watercourse (L – lowlands, H – highlands, M – mountains), parameters of the empirical sample (Skew. is the empirical skewness, Kurt. is the empirical kurtosis and 4thMoment is the 4th center moment); sample size (N).

The first two axes (RDA 1 and RDA 2) explain 46.61% of the variance (38.71% and 7.90%, respectively) (Fig. S3a). The Q_p and A are strongly correlated with RDA 1 and so is Kurt. with RDA 2. According to the response variables, scale and location are related to RDA 1, and shape is related to RDA 2. Scale and location are strongly positively correlated with Q_p (scores 0.98) and A (scores 0.64) (Fig. S3a). The shape parameter of LN3 in FFA has been found to be correlated with extreme flows and the catchment area (Haktanir and Horlacher, 1993; Smith, 1989).

The shape is negatively related to Kurt. (scores -0.55) and H (scores -0.51) (Fig. S3a). The shape is inversely proportional to N (scores 0.37) (Fig. S3a). Location is weakly correlated to NMT (scores 0.2) (Fig. S3a). The shape is weakly correlated to N (scores 0.37) and inversely proportional to H (scores –

0.51). The PT (scores 0.21), NT (scores -0.28), M (scores 0.2), L (scores -0.56) is correlated with RDA 3 (Fig. S3a).

In the second RDA, the first two axes (RDA 1 and RDA 2) explain 54.09% of the variance (38.98% and 15.11%, respectively) (Fig. S3b). The Qp, and A are strongly correlated with RDA 1 and so is Skew. with RDA 2. According to the response variables, scale and location are related to RDA 1, and shape is related to RDA 2. Scale and location are strongly positively correlated with Qp (scores 0.98) and A (scores 0.65) (Fig. S3b). The shape is negatively related to Skew. (scores -0.85) and H (scores -0.39) (Fig. S3b). The location is weakly inversely proportional to N (scores 0.33) (Fig. S3b). Location is weakly correlation to NMT (scores 0.2) (Fig. S3b). The PT (scores 0.18), NT (scores -0.22), and M (scores 0.2), L (scores -0.39) are correlated with RDA 3 (Fig. S3b).

In the Third RDA, the first two axes (RDA 1 and RDA 2) explain 57.72% of the variance (42.60% and 15.12%, respectively) (Fig. S3c). The Qp, (e) and 4thMoment are strongly correlated with RDA 1 and Skew. with RDA 2 (Fig. S3c). According to the response variables, scale and location are related to RDA 1, and shape is related to RDA 2 (Fig. S3c). Scale is strongly positively correlated with (e) and location is strongly positively correlated with Qp and 4thMoment (Fig. S3c). The shape is negatively related to Skew. and weakly correlated with H, while positively with (d). Location is negatively correlated with NT (Fig. S3c). Scale is negatively correlated with (b) and (c), while positively correlated with N (Fig. S3c). As reported (Kamal et al., 2017) the larger the N, the better the result for LN3. Moreover, M, L, NMT and PT do not influence the distribution parameters (Fig. S3c).

4.4.4 Pearson type III distribution (P3)

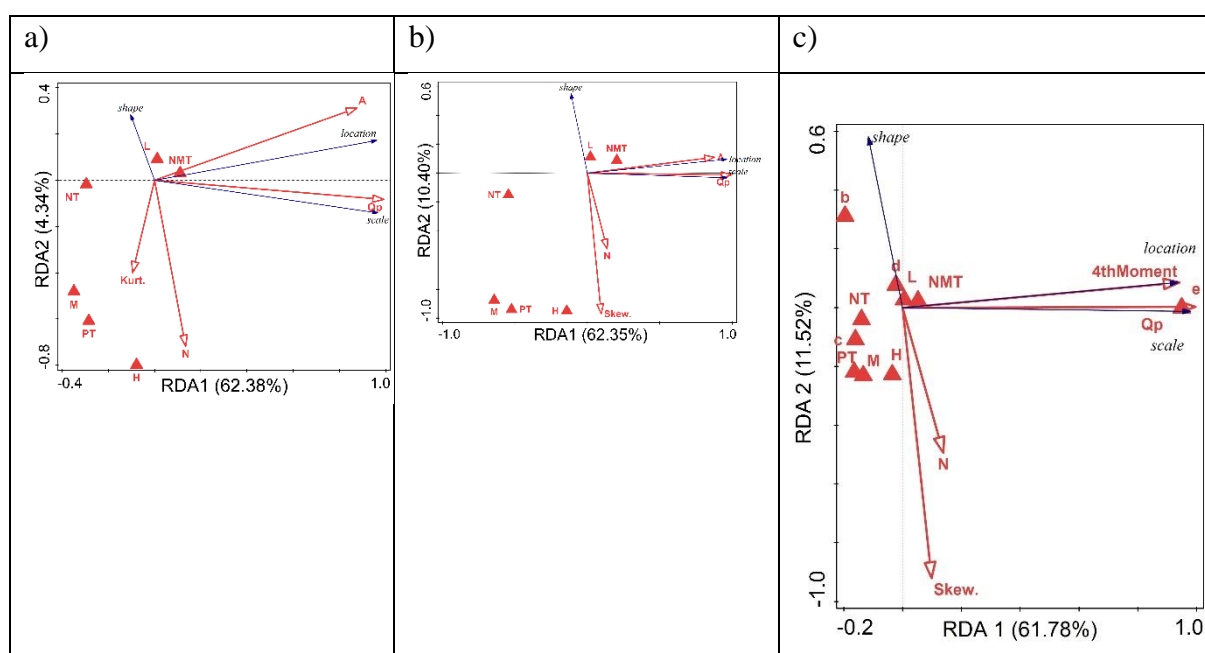


Fig. S4. Redundancy analysis (RDA) of the relation between environmental variables and sample characteristics and the parameters of P3 (scale, shape, add. shape, location). Descriptions of symbols: catchment area ranges (in km²): a –

<10, b – 10-100, c – 100-1000, d – 1000-10000, e – > 10000; flow peak (Q_p); trend (NMT is no trend, PT is positive trend and NT is negative trend); the nature of the watercourse (L – lowlands, H – highlands, M – mountains), parameters of the empirical sample (Skew. is the empirical skewness, Kurt. is the empirical kurtosis and 4thMoment is the 4th center moment); sample size (N).

The first two axes (RDA 1 and RDA 2) explain 66.72% of the variance (62.38% and 4.34%, respectively) (Fig. S4a). The Q_p, and A are strongly correlated with RDA 1 and so is N with RDA 2. According to the response variables, scale and location are related to RDA 1, and shape is related to RDA 2. Scale is strongly positively correlated with Q_p (scores 0.99) and Location is strongly positively correlated with A (scores 0.88) (Fig. S4a). This contrasts with the findings of Hebson and Wood (1986); Hu et al. (2020), Farooq et al. (2018), Flynn et al. (2006); Ribeiro-Correa and Rousselle (1993), who concluded that the scale parameter of P3 is indeed strongly correlated with increasing catchment area in FFA.

The shape is strongly negatively correlated with N (scores -0.72) (Fig. S4a). In turn, the shape is weakly negatively correlated with Kurt. (score -0.4) and H (score -0.26). The shape is weakly positively correlated with L (score 0.27) (Fig. S4a). The M (scores 0.08), NT (scores -0.17), PT (scores 0.12), NMT (scores -0.22) are all correlated with RDA 3 (Fig. S4a).

In the second RDA, the first two axes (RDA 1 and RDA 2) explain 66.72% of the variance (62.35% and 10.40%, respectively) (Fig. S4b). The Q_p, and A are strongly correlated with RDA 1 and Skew. and N are strongly correlated with RDA 2. According to the response variables, scale and location are related to RDA 1, and shape is related to RDA 2. Scale is strongly positively correlated with Q_p (scores 0.99) and location is strongly positively correlated with A (scores 0.88) (Fig. S4a). The shape is strongly negatively correlated with both Skew. (score -0.97) and N (scores -0.52) (Fig. S4a). The shape is weakly negatively correlated with H (score -0.17) and M (score -0.04) and PT (score -0.09). The shape is weakly positively correlated with L (score 0.17) (Fig. S4a). The NMT (scores 0.18) and NT (scores -0.17) are weakly correlated with location (Fig. S4a).

In the third RDA, the first two axes (RDA 1 and RDA 2) explain 73.30% of the variance (61.78% and 11.52%, respectively) (Fig. S4c). The Q_p, 4thMoment and (e) are strongly correlated with RDA 1 and so is Skew. with RDA 2. According to the response variables, scale and location are related to RDA 1, and shape is related to RDA 2 (Fig. S4c). Scale is strongly positively correlated with Q_p and location is strongly positively correlated with (e) and 4thMoment (Fig. S4c). In contrast to the results shown in Fig. S4a-b Hebson and Wood, 1986; Hu et al., 2020, Farooq et al., 2018; Flynn et al., 2006; Ribeiro-Correa and Rousselle, 1993 came to the same conclusions, stating that the scale parameter of the P3 is indeed strongly correlated with the increasing catchment area in flood frequency analysis.

The larger the Q_p , the greater the scale, and the larger the 4thMoment – especially for the largest catchments (e) – the greater the location (Fig. S4c). In the current analysis, Q_p and MAF are strongly correlated with the scale (Fig. S5-S6).

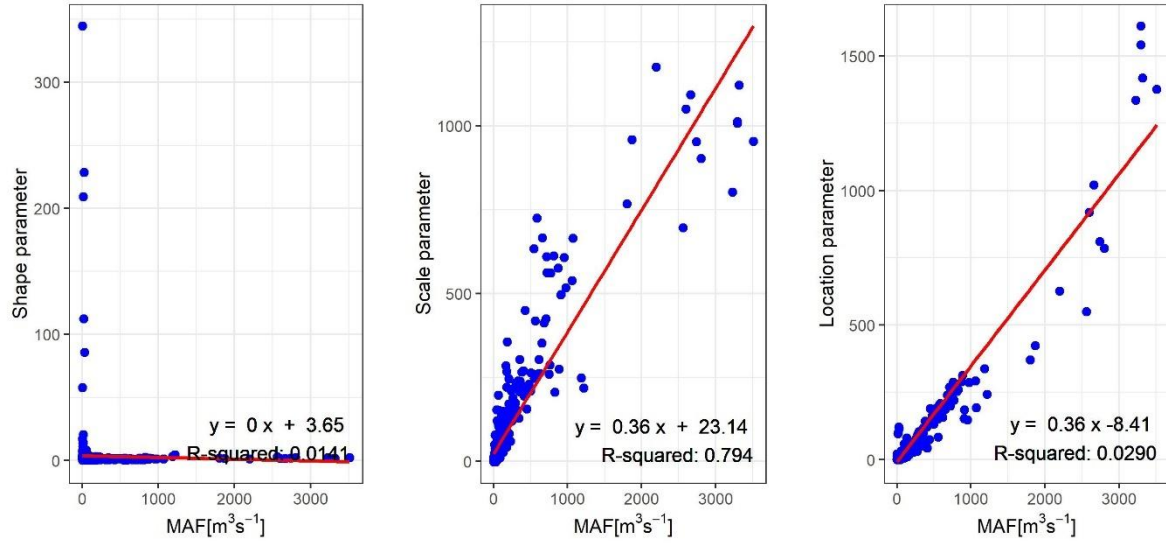


Fig. S5. Scatter plots of the P3 parameters and the predictor variable MAF.

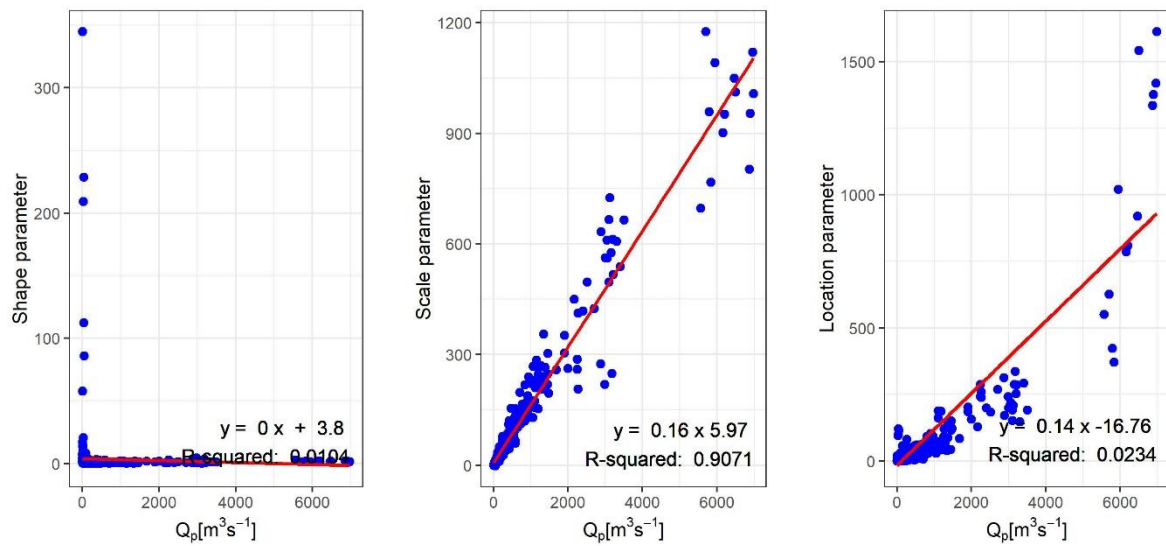


Fig. S6. Scatter plots of the P3 parameters and the predictor variable Q_p .

350 The location parameter of the log-Pearson type III in flood frequency analysis is not significantly correlated with flows, trends, landscape, or sample size (Hu 2019) (Hu et al., 2020), , which is consistent with current findings. However, as noted by Hu et al. (2020), the location parameter of the P3 distribution is also not significantly correlated with the catchment area. Our findings confirm this, but also show that it is positively and significantly correlated only with large catchments ($A > 10000$).

The shape parameter is inversely proportional to Skewn. and N (Fig. S4c). This means that with smaller sample sizes and lower Skewn., the shape parameter is larger. As reported by Hu et al. (2020), Skewn. in the log-Pearson Type III distribution is very sensitive to N. On the other hand, Jia et al. (2023) found that using trimmed L-moments methods for P3 in flood frequency analysis allowed for good parameter estimation even for samples with small sizes and skewness greater than twice the coefficient of variation.

360 The parameters (b) and (d) have a weak positive relation to the shape parameter (Fig. S4c). In catchments (b) and (d), the shape parameter increases. The location parameter is weakly negatively correlated with (c) and PT (Fig. S4c). Catchments (c) and detected PT lead to a decrease in the location parameter (Fig. S4c). In contrast, H, L, M, NT, and NMT do not influence the distribution parameters (Fig. S4c). Thus, distribution parameters are not sensitive to landscape forms or the absence of trends or negative trends. This contrasts with the findings of Farooq et al.(2018) Jain and Singh (1987), Vogel and McMartin (1991), who concluded that the shape parameter of the Pearson type III distribution is strongly correlated with the NMT in FFA. Moreover, Valeo and Rasmussen (2000), who investigated the log-Pearson Type III distribution, state that not only the catchment area as an independent variable determines the Qp rate, but also the topographical distribution.

370 Konrad (2021) highlighted the importance of understanding trends in annual peak streamflow, particularly for the median annual flood, which can be influenced by factors such as reservoir operation and urban development (Konrad and Restivo, 2021).

The following points summarize key findings regarding the relationships between environmental factors and the parameters of various probability distributions, as analyzed within the context of RDA:

- The GGEV and P3 distributions tend to have the parameters H, M, L located outside of RDA1.
- GGEV and P3 share a common feature of a negative correlation between N and shape, while GEV and LN3 exhibit more complex correlation patterns.
- GGEV, GEV, and LN3 show similar correlations between the parameters A, c, and e in the context of RDA1, whereas P3 differs in this respect.
- GGEV and GEV share a pattern where NMT appears in RDA2. LN3 shows a broader presence in RDA1 and RDA2, while P3 has a different configuration.
- The pattern for GGEV differs from the other distributions because, in GEV, LN3, and P3, skewness is distinctly concentrated only in RDA2.

Based on the above comparison, the GGEV distribution shows some similarities with other distributions regarding the occurrence and correlation of parameters in the RDA analysis. However, these differences in certain aspects, such as the distribution of parameters in the principal components and parameter correlations, indicate unique characteristics of GGEV compared to GEV, LN3, and P3. GGEV often

differs from other distributions in how its parameters spread within the principal component space,
which may be significant when modeling and interpreting data analysis results.

References

Ahilan, S., O’Sullivan, J. J., and Bruen, M.: Influences on flood frequency distributions in Irish river catchments, *Hydrol. Earth Syst. Sci.*, 16, 1137–1150, <https://doi.org/10.5194/hess-16-1137-2012>, 2012.

Arnaud, P., Lavabre, J., Fouchier, C., Diss, S., and Javelle, P.: Sensitivity of hydrological models to uncertainty in rainfall input, *Hydrological Sciences Journal*, 56, 397–410, <https://doi.org/10.1080/02626667.2011.563742>, 2011.

Balbi, M. and Lallemand, D. C. B.: The Cost of Imperfect Knowledge: How Epistemic Uncertainties Influence Flood Hazard Assessments, *Water Resources Research*, 59, e2023WR035685, <https://doi.org/10.1029/2023WR035685>, 2023.

Ekanayake, S. T. and Cruise, J. F.: Comparisons of Weibull- and exponential-based partial duration stochastic flood models, *Stochastic Hydrol Hydraul*, 7, 283–297, <https://doi.org/10.1007/BF01581616>, 1993.

Farooq, M., Shafique, M., and Khattak, M. S.: Flood frequency analysis of river swat using Log Pearson type 3, Generalized Extreme Value, Normal, and Gumbel Max distribution methods, *Arab J Geosci*, 11, 216, <https://doi.org/10.1007/s12517-018-3553-z>, 2018.

Flynn, K. M., William H. Kirby, and Paul R. Hummel: User’s Manual for Program PeakFQ, Annual Flood-Frequency Analysis Using Bulletin 17B Guidelines, 2006.

Haktanir, T. and Horlacher, H. B.: Evaluation of various distributions for flood frequency analysis, *Hydrological Sciences Journal*, 38, 15–32, <https://doi.org/10.1080/02626669309492637>, 1993.

He, J., Anderson, A., and Valeo, C.: Bias compensation in flood frequency analysis, *Hydrological Sciences Journal*, 60, 381–401, <https://doi.org/10.1080/02626667.2014.885651>, 2015.

Hebson, C. S. and Wood, E. F.: A Study of Scale Effects in Flood Frequency Response, in: *Scale Problems in Hydrology*, vol. 6, edited by: Gupta, V. K., Rodríguez-Iturbe, I., and Wood, E. F., Springer Netherlands, Dordrecht, 133–158, https://doi.org/10.1007/978-94-009-4678-1_7, 1986.

Hu, L., Nikolopoulos, E. I., Marra, F., and Anagnostou, E. N.: Sensitivity of flood frequency analysis to data record, statistical model, and parameter estimation methods: An evaluation over the contiguous United States, *J Flood Risk Management*, 13, e12580, <https://doi.org/10.1111/jfr3.12580>, 2020.

Jain, D. and Singh, V. P.: Comparison of Some Flood Frequency Distributions Using Empirical Data, in: *Hydrologic Frequency Modeling*, edited by: Singh, V. P., Springer Netherlands, Dordrecht, 467–485, https://doi.org/10.1007/978-94-009-3953-0_33, 1987.

Kamal, V., Mukherjee, S., Singh, P., Sen, R., Vishwakarma, C. A., Sajadi, P., Asthana, H., and Rena, V.: Flood frequency analysis of Ganga river at Haridwar and Garhmukteshwar, *Appl Water Sci*, 7, 1979–1986, <https://doi.org/10.1007/s13201-016-0378-3>, 2017.

430 Konrad, C. and Restivo, D.: Assessment and significance of the frequency domain for trends in annual peak streamflow, *J Flood Risk Management*, 14, e12761, <https://doi.org/10.1111/jfr3.12761>, 2021.

Kuczera, G.: Robust flood frequency models, *Water Resources Research*, 18, 315–324, <https://doi.org/10.1029/WR018i002p00315>, 1982.

Morrison, J. E. and Smith, J. A.: Stochastic modeling of flood peaks using the generalized extreme value distribution, *Water Resources Research*, 38, <https://doi.org/10.1029/2001WR000502>, 2002.

Nascimento, F., Bourguignon, M., and Leao, J.: Extended generalized extreme value distribution with applications in environmental data, *HJMS*, 46, 1–1, <https://doi.org/10.15672/HJMS.20159514081>, 2015.

440 Northrop, P. J.: Likelihood-based approaches to flood frequency estimation, *Journal of Hydrology*, 292, 96–113, <https://doi.org/10.1016/j.jhydrol.2003.12.031>, 2004.

Ribeiro-Correa, J. and Rousselle, J.: A hierarchical and empirical Bayes Approach for the regional Pearson type III distribution, *Water Resources Research*, 29, 435–444, <https://doi.org/10.1029/92WR02086>, 1993.

Roodsari, B. K. and Chandler, D. G.: Distribution of surface imperviousness in small urban catchments predicts runoff peak flows and stream flashiness, *Hydrological Processes*, 31, 2990–3002, <https://doi.org/10.1002/hyp.11230>, 2017.

450 Sampaio, J. and Costa, V.: Bayesian regional flood frequency analysis with GEV hierarchical models under spatial dependency structures, *Hydrological Sciences Journal*, 66, 422–433, <https://doi.org/10.1080/02626667.2021.1873997>, 2021.

Smith, J. A.: Regional flood frequency analysis using extreme order statistics of the annual peak record, *Water Resources Research*, 25, 311–317, <https://doi.org/10.1029/WR025i002p00311>, 1989.

Tabari, H., Moghtaderi Asr, N., and Willems, P.: Developing a framework for attribution analysis of urban pluvial flooding to human-induced climate impacts, *Journal of Hydrology*, 598, 126352, <https://doi.org/10.1016/j.jhydrol.2021.126352>, 2021.

460 Tyralis, H., Papacharalampous, G., and Tantanee, S.: How to explain and predict the shape parameter of the generalized extreme value distribution of streamflow extremes using a big dataset, *Journal of Hydrology*, 574, 628–645, <https://doi.org/10.1016/j.jhydrol.2019.04.070>, 2019.

Valeo, C. and Rasmussen, P.: Topographic Influences on Flood Frequency Analyses, *Canadian Water Resources Journal*, 25, 387–406, <https://doi.org/10.4296/cwrj2504387>, 2000.

Villarini, G. and Smith, J. A.: Flood peak distributions for the eastern United States, *Water Resources Research*, 46, 2009WR008395, <https://doi.org/10.1029/2009WR008395>, 2010.

Vogel, R. W. and McMartin, D. E.: Probability Plot Goodness-of-Fit and Skewness Estimation Procedures for the Pearson Type 3 Distribution, *Water Resources Research*, 27, 3149–3158, <https://doi.org/10.1029/91WR02116>, 1991.

470 Willems, P., Guillou, A., and Beirlant, J.: Bias correction in hydrologic GPD based extreme value analysis by means of a slowly varying function, *Journal of Hydrology*, 338, 221–236, <https://doi.org/10.1016/j.jhydrol.2007.02.035>, 2007.

Willems, P., Nyeko, P. O., Francis, M., and Gamal, A.: Regional Flood Frequency Analysis for the River Nile Basin, in: *Proceedings of the International Conference of UNESCO Flanders fit, FRIEND/Nile Project, Towards a Better Cooperation*, Sharm El-Sheikh, Egypt, 555–570, 12–14 November.